ISSN 1063-7745, Crystallography Reports, 2021, Vol. 66, No. 6, pp. 897–905. © Pleiades Publishing, Inc., 2021.

DIFFRACTION AND SCATTERING OF IONIZING RADIATIONS

X-Ray Diffraction Interferometer with One Slit: Computer Simulations and Analytics

V. G. Kohn[a] and I. A. Smirnova[b,*]

[a] *National Research Centre "Kurchatov Institute," Moscow, 123182 Russia*

[b] *Institute of Solid State Physics, Russian Academy of Sciences, Chernogolovka, Moscow oblast, 142432 Russia*

**e-mail: irina@issp.ac.ru*

Received March 17, 2021; revised March 17, 2021; accepted April 7, 2021

Abstract—A theoretical basis and a method of accurate computer simulations for studying the properties of X-ray diffraction interferometer with one slit are formulated. The slit serves as a secondary source of coherent divergent radiation, while the direct and reflected beams are split in space in a narrow gap between two crystal blocks. The theory is formulated for an arbitrary distance between the secondary source and a detector. Two most interesting cases are investigated in detail. It the first case the effect of diffraction focusing is realized for a thickness of the first crystal at a relatively large distance. This case is equivalent to a two-slit interferometer. In the second case, the distance is minimal, and thicknesses of the two blocks are equal. Here, an interference pattern can be obtained at a less total thickness of the blocks, and the experimental scheme is more compact. Analytical formulas for the interference fringe period and the beam widths under the Borrmann effect are derived.

DOI: 10.1134/S1063774521060195

INTRODUCTION

Optical interferometers have been applied for more than two centuries in various measurements to solve both practical and scientific problems [1]. To date, interferometers of different types have been designed; however, the first two-slit interferometer (known as the Young interferometer) has become most popular. In the case of diffraction from a slit with width d, monochromatic radiation with a wavelength λ acquires angular divergence with a width $\alpha = \lambda/d$ even if a plane wave is incident on the slit. At diffraction from two slits, the related beams begin to intersect at a distance $z_0 = x_0/\alpha$ along the optical axis, where x_0 is the distance between the slits in the transverse direction. If coherent radiation passes through the slits, the phase relations in different beams are consistent, and interference fringes with a period $p = \lambda z_1/x_0$ ($z_1 > z_0$ is the distance from the slits to the detector) arise upon addition of two fields.

For X-rays, the development of this interferometry has been hindered for a long time in view of the absence of coherent sources (i.e., rather small coherence length and insufficient radiation brightness). The situation changed in the middle of the 1990s with the development of third-generation synchrotron radiation (SR) sources (the first was designed in Grenoble, France). Currently, there are many publications on X-ray interferometry of different types. We should note studies [2–7], where the most interesting interferometers based on compound refractive lenses [8] were tested.

At the same time, X-ray optics provides a possibility of radically new interferometry based on X-ray diffraction in single crystals [9]. A necessary condition for operation of two-slit interferometer is as follows: the beams must have sufficiently a high angular divergence and intersect at a distance as small as possible. For X rays in a standard Young interferometer, this condition is difficult to fulfill because of the very small wavelength λ.

At the same time, it is known that, in the case of two-wave diffraction in a single crystal, a beam bounded by a narrow slit exposes the so-called Borrmann fan with an angle $2\theta_B$; θ_B is the Bragg angle, which may take any value from 0 to 90°. This fact was experimentally found for the first time in [10] and theoretically explained in [11, 12]. Note that the beams from two slits can interfere in a crystal with a thickness smaller than 1 mm, forming periodic fringes with high and low intensities.

Diffraction interferometry from two slits (i.e., an analog of the Young interferometer, but implemented in a single crystal) was investigated theoretically in [13], where an analytical formula for the interference fringe period was obtained: $p = 2\Lambda\, t \tan^2(\theta_B)/x_0$ (x_0 is the distance between the slits, $\Lambda = \lambda\cos(\theta_B)/|\chi_h|$ is the extinction length, χ_h is the diffraction parameter, and t is the crystal thickness). The parameters p and x_0 are

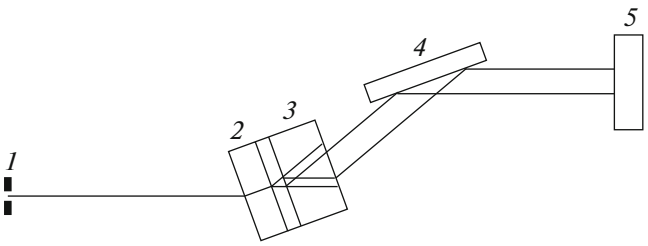

Fig. 1. Scheme of the suggested experiment: (*1*) secondary source in the form of slit, (*2*) first crystal, (*3*) second crystal, (*4*) crystal for changing the reflected-beam direction, and (*5*) detector.

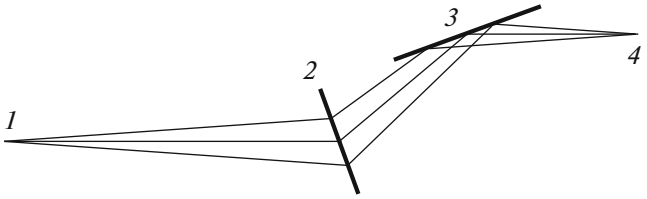

Fig. 2. Scheme illustrating the operation of polychromatic focusing: (*1*) source of a spherical wave, (*2*) crystal in the Laue reflection position, (*3*) crystal in the Bragg reflection position, and (*4*) observation point.

measured in the direction parallel to the crystal surface.

Although this statement of experiment deserves attention, we should note its drawbacks. First, in any experiment with two slits only a very small part of the incident beam is used and, therefore, the light-gathering power is low. Second, this scheme is spectrally unstable if the distance Z between the slits and the detector is not too small, i.e., it requires very high monochromaticity of radiation. Note also that another slit with a size smaller than the coherence length should be placed before the two slits. The fraction of coherent radiation in modern SR sources can often be increased only by reducing the beam angular divergence. However, such a beam cannot pass through two slits and should be diverged anyway. If the beam is wide, its coherence length is generally small, and a slit must be used to select coherent radiation.

It is of interest that an interferometer without two slits can be designed. One slit is sufficient for either diverging a beam or selecting its coherent part. The point is that, first, the diffraction in a crystal forms simultaneously two beams (direct and reflected) and, second, the diffraction focusing effect is present. This effect was theoretically predicted in [14, 15] and experimentally discovered right away in [16–18]. Later this effect was investigated in [19, 20] for the case of diffraction from two successive crystals spaced by a large distance. As was shown in the first study [14] and in subsequent works [21–24], for a specified crystal thickness t, a spherical wave from a secondary source with small transverse sizes is focused at a certain distance between the source and detector, $Z = tF_B/|\chi_h|$, where $F_B = \sin\theta_B \sin(2\theta_B)$, in both the direct and reflected beams.

Focusing occurs at a sufficiently large crystal thickness t_1, when the Borrmann effect is additionally present. The essence of this effect is that the absorption coefficient is many times lower for a part of radiation and only this part can pass through the crystal, both in the forward and reflected directions. Specifically this part undergoes focusing, which occurs equally in both beams, and the wave functions have an identical phase. At the crystal output, two almost identical beams with a very small transverse width propagate (each in its own direction) and are split in space at a distance of $2t_g\sin(\theta_B)$ in the direction perpendicular to each beam (t_g is the air gap thickness).

If the second crystal with thickness t_2 is placed in their way, each of them will diffract again, exposing a region in the crystal in the form of a Borrmann fan; the intersection of these regions leads to interference. The only difference from the experimental scheme with two slits that was considered in [13] is that the direct beam will diffract on the reciprocal lattice vector **h** (as in the first crystal), whereas the reflected beam will diffract on the vector –**h**. This situation is illustrated in Fig. 1, where crystal *2* focuses the beams, which interfere in crystal *3*. Crystal *4* is required only to change the reflected beam direction to the initial, which is important for operation on SR sources.

An advantage of this scheme is the possibility of polychromatic focusing effect for the reflected beam, which was described in [25]. This focusing is implemented at equal distances from the interferometer to the source and the detector. Correspondingly, the interference pattern has spectral stability; i.e., the interference effect can be observed at a rather moderate SR monochromatization. The polychromatic focusing effect is illustrated in Fig. 2. Let the divergent beam from point *1* be incident on crystal *2* to implement Laue diffraction. For a specified wavelength λ, the crystal is oriented so that the Bragg angle θ_B corresponds to the horizontal beam (the intermediate beam in Fig. 2). It is reflected by angle $2\theta_B$ and, falling on crystal *3*, is reflected again (in the initial direction).

The Bragg angle decreases with a decrease in wavelength. Note that the diffraction condition is now satisfied for the lower beam in Fig. 2 and in another region of the crystal. After reflection in crystal *3*, this beam becomes the upper one and, at point *4*, it arrives at the same point on the detector as the first (horizontal) beam. The situation is the same with the increase in the wavelength. In other words, all waves in the wavelength range in which reflection from crystal *3* may occur arrive at the detector at the same point. Hence, interference fringes can clearly be seen, and the contrast is not deteriorated.

Another advantage is that splitting of beams in space occurs in this interferometer after their diffraction focusing, which does not lead to intensity loss; i.e., this scheme has a high light-gathering power. The above-described scheme is also of interest. It is proposed for the first time in this study.

However, as a more thorough analysis showed, it is not necessary to focus beams at the end of the first crystal. The main features of the new interferometer are the splitting of beams in space (i.e., in an air interlayer between the first and second crystals) and the Borrmann effect (i.e., the selection of only one field, which is weakly absorbed, out of two). One can also consider other schemes; note that the interference occurs at an arbitrary distance Z between the secondary source (e.g., slit) and the detector. If this distance tends to zero (specifically, is sufficiently small), the most clear interference occurs at equal thicknesses of the first and second crystals.

In this study, we present the fundamentals of the theory and the method of numerical calculation of interference pattern in the above-described interferometer at an arbitrary relation between the distance Z, crystal thicknesses, and the air-layer thickness; the results of calculating the specific values of the parameters; and the analytical formulas derived for the oscillation period and beam width.

THEORETICAL FUNDAMENTALS AND METHOD OF COMPUTER SIMULATIONS

It was shown in [11, 14] that it is most convenient to compute the X-ray diffraction in crystals by the Fourier transform method. In the general form, this method is as follows. First, the wave function (WF) of X rays at the detector is calculated in the absence of crystals (i.e., in real space and in the (x, z) diffraction plane). The z axis is directed along the beam (from the source to the detector), and the x axis is directed perpendicularly (across the beam). The distance between the secondary source and detector is Z.

Then, this WF at the detector $E_0^{(0)}(x)$ is presented as an integral over plane waves, i.e., the Fourier transform $E_0^{(0)}(q)$ is calculated. Since a reflected (diffracted) wave arises in the crystal upon diffraction, it is convenient to take this circumstance into account at the very beginning and introduce the wave-function vector composed of two components: $E_0^{(0)}(q)$ and $E_1^{(0)}(q)$. Note that initially $E_1^{(0)}(q) = 0$. The solution to the problem of plane wave diffraction in a plate-shaped crystal with a thickness t_1 was obtained long ago; it can be found in textbooks (see, e.g., [26–28]).

This solution can be presented as a multiplication of the matrix $M_{ik}(q, t_1)$ by the vector $E_k(q)$, where subscripts i and k take two values (0 or 1). Thus, the solution at the detector $E_i^{(1)}(q)$ in the presence of one crystal with a thickness t_1 on the beam path can be written in the form

$$E_i^{(1)}(q) = M_{ik}^{(1)}(q, t_1)E_k^{(0)}(q). \quad (1)$$

From here on, double subscripts indicate summation.

If there are several crystals on the beam pass, which are tightly pressed against each other, one should additionally perform multiplication for the second crystal with a thickness t_2:

$$E_i^{(2)}(q) = M_{ik}^{(2)}(q, t_2)E_k^{(1)}(q), \quad (2)$$

and so on for each next crystal. A layer of amorphous material or just air may be located on the beam path instead of a crystal. Such layers are also described by the matrix $M_{ik}(q, t)$ of special form. However, to make this approach valid, it is suggested that the total thickness of this complex is not too large. This is obvious for crystals, because they absorb. For air layers, this suggestion follows from the structure of the matrix in use, because it is derived on the assumption of geometric optics validity.

After carrying out multiplications for all layers, one performs an inverse Fourier transform and obtains a result in real space again (i.e., at the detector in the diffraction plane, but with allowance for the system of crystals). It is clear from the above-described calculation technique that the system of crystals can be located at any place between the secondary source and detector, because their position does not affect the result if a symmetric reflection is used. In other words, the observed interference pattern depends on only the total distance Z. The crystals do not affect this distance.

In this study, we apply the general method to the experimental scheme shown in Fig. 1. The secondary radiation source is a narrow slit with a width d, on which a plane wave is incident. The slit may have either sharp or smoothed edges (this factor is easily taken into account in the calculation). There is nothing between the slit and detector, except for crystals. The diffraction from a slit with sharp edges is calculated analytically. However, for generality, we will consider the numerical method, which is convenient for solving the above-considered problem of taking into account the crystals.

Let the slit in real space be described by the WF $\psi(x)$. We calculate the Fourier transform $\psi(q)$, and then the Fourier transform of the WF at the detector can be written as

$$E_0^{(0)}(q) = C_1P(q, Z)\psi(q), \quad C_1 = (\lambda Z)^{1/2}, \quad (3)$$

where a normalization factor C_1 is introduced and

$$P(q, Z) = \exp(-i\lambda Zq^2/4\pi) \quad (4)$$

is the Fourier transform of the Fresnel propagator. At this statement of the problem, we obtain $E_0^{(0)}(q)$ at

once, whereas inverse Fourier transform should be performed to calculate $E_0^{(0)}(x)$. However, one can deal without it, if X-ray diffraction in crystals is of interest. Multiplications shown in formulas (1) and (2) can be performed immediately.

Below, the formulas for calculating the matrix $M_{ik}(q, t)$ in the case of symmetric Laue diffraction are presented:

$$M_{00}(q,t) = U[E_p + r^2 E_m],$$
$$M_{10}(q,t) = X_h V[E_p - E_m], \quad (5)$$

$$M_{01}(q,t) = X_{-h} V[E_p - E_m],$$
$$M_{11}(q,t) = U[r^2 E_p + E_m], \quad (6)$$

where

$$U = (1 + r^2)^{-1}, \quad E_p = \exp(A + G),$$
$$E_m = \exp(A - G), \quad V = (2g)^{-1}, \quad (7)$$

$$A = i[X_0 + \alpha_q]t/(2\gamma_0), \quad G = igt/(2\gamma_0),$$
$$g = (\alpha_q^2 + X^2)^{1/2}, \quad (8)$$

$$X^2 = X_h X_{-h}, \quad r = (\alpha_q + g)/X,$$
$$X_{0,h,-h} = K\chi_{0,h,-h}, \quad (9)$$

$$\alpha_q = (q - q_0)\sin(2\theta_B), \quad \gamma_0 = \cos(\theta_B). \quad (10)$$

Here, the parameter g has a positive imaginary part by definition; χ_0, χ_h, and χ_{-h} are the diffraction parameters, which are Fourier components of the crystal polarizability at the reciprocal lattice vectors 0, **h**, and **−h**, respectively; θ_B is the Bragg angle; $K = 2\pi/\lambda$; and the parameter $q_0 = K\theta_0$ describes possible deviation of the crystal angular position from the Bragg angle.

Note that the diffraction matrix $M_{ik}(q, t)$, determined from formulas (5)–(10), shows the angular dependence of the intensity at plane-wave diffraction in the crystal in such a form that the curves tend gradually to a constant or to zero in their tails (i.e., at $|q| \gg X$). This is convenient for plotting the functions. However, when calculating the Fourier transform, the diffraction region (Borrmann fan) is located on the left from the origin of coordinates, and this point corresponds to the beam passage from the point source along the incident-wave direction, which is inconvenient.

The situation is more convenient when the Borrmann fan is located symmetrically on the left and on the right from the coordinate origin. In other words, the coordinate origin should be shifted along the x axis so as to be in the middle of the Borrmann fan. An additional shift by a distance $x_s = -Z\theta_0$ should be performed for a finite distance Z to correct the change in the Bragg direction at an angular displacement of crystal. A correct choice of the beam center is especially important for a thick crystal, because only the part of the beam corresponding to the middle of the Borrmann fan passes through the crystal in this case (because of the Borrmann effect). The coordinate origin is shifted in the program by multiplication (before carrying out a Fourier transform) of the integrand function by the factor

$$F(q) = \exp(iq[Z\theta_0 - t\sin(\theta_B)]). \quad (11)$$

Nevertheless, the experimental scheme presented in Fig. 1 should satisfy some additional requirements. The point is that the most interesting interference pattern occurs in the reflected beam if the polychromatic focusing condition is satisfied, when the distances before and after the interferometer are equal. Note that the distance between the interferometer and detector cannot be small if the diffraction focusing effect is used for a relatively thick crystal.

As a consequence of these conditions, the reflected beam at the detector can be significantly deflected in the transverse direction from the optical axis. Since SR sources provide little place in the transverse direction, these beam deflections should be corrected by additional reflection by the same angle in the reverse direction. To this end (as is shown in Fig. 1), one should use a Bragg reflection from a thick crystal, because a Laue reflection would violate the polychromatic focusing condition, in contrast to Bragg reflection (Fig. 2).

As the calculations show, an additional symmetric Bragg reflection from crystal *4* in Fig. 1 barely deteriorates the interference pattern at a correct angular position of the crystal. The symmetric Bragg reflection amplitude for a thick crystal with an inversion center is also well known. We present it to show the formula that was used in the calculation:

$$M_B(q) = (\sigma + a)/s, \quad \sigma = (q - q_1)\sin(2\theta_B) - i\mu_0, \quad (12)$$

$$a = (\sigma^2 - s^2)^{1/2}, \quad s = K\chi_h, \quad \mu_0 = K\,\mathrm{Im}(\chi_0). \quad (13)$$

Here, the imaginary part of parameter a is by definition larger than zero. Therefore, at large $|q|$ values we find that a is approximately equal to $-\sigma$ and $M_B(q)$ tends to zero. In addition, $q_1 = K\varphi$, where φ is the angle of possible crystal deviation from the exact diffraction position.

It is known [26–28] that, under conditions of Bragg reflection, the center of the angular reflection region is shifted by $-\mathrm{Re}(\chi_0)/\sin(2\theta_B)$ if the crystal is aligned strictly at the Bragg angle. This displacement can be compensated by an additional crystal rotation. It is assumed in formulas (12) and (13) that this compensation has already been done, and the condition $q_1 = 0$ corresponds to the crystal position where the center of the angular reflection region is at the point $q = 0$. Specifically this position of the reflector crystal minimally deteriorates the interference pattern.

Formulas (1)–(13) were used to write a computer program for calculating the intensity distribution in space before the detector at diffraction from two crystals with thicknesses t_1 and t_2, separated by an air layer with a thickness t_g, and possible additional reflection of the reflected beam in the direction of the forward beam. The diffraction parameters were calculated using the on-line program [29].

The computer program was written in the ACL language [30]. Fourier integrals were calculated using the fast Fourier transform (FFT) procedure [31], built in the ACL. The code of this procedure in FORTRAN has been known since the middle of the last century as a part of the NAG library [32]. The calculations were performed for the number of points $N = 16384$. The point-grid step d_x is specified, and the step $d_q = Kd_\theta = 2\pi/(Nd_x)$ and size Nd_q of the computational box in reciprocal space should be sufficiently large to make the integrand function zero at the edges of the region.

RESULTS AND DISCUSSION

The developed program makes it possible to calculate the angular dependence of intensity for the plane-wave diffraction and different geometries of spherical-wave diffraction. One can easily check an evident result: if the air layer thickness is $t_g = 0$ and the first and second crystals have identical structures and atomic compositions, the calculation result for two crystals coincides with that for one crystal with the total thickness $2t = t_1 + t_2$.

In this study, we present the calculation results for two cases. The first one corresponds to the diffraction focusing in the first crystal. This case is similar to Balyan's interferometer [13]. Here, the first-crystal thickness t_1 corresponds to the radiation focusing in the detector plane in the absence of second crystal. At some distance after the second crystal output, the beams diverge in space, and each wave should be considered independently. It is easy to understand that the doubly transmitted and doubly reflected waves interfere in the direct beam, whereas the first transmitted and then reflected and the first reflected and then transmitted waves interfere in the reflected beam.

Accordingly, we obtain an asymmetric pattern in the direct beam and a symmetric pattern in the reflected beam. Figure 3 shows the result of calculating the interference pattern in the reflected beam with a change in the second-crystal thickness, without reflection from the third crystal, for following parameters: slit size $d = 5$ μm, distance $Z = 5$ m, Ge crystal, reflection 220, photon energy 25 keV ($\lambda = 0.0496$ nm), first-crystal thickness $t_1 = 0.4$ mm, and air layer thickness $t_g = 0.25$ mm. The range of variation in the second-crystal thicknesses t_3 from 0.55 to 1.15 mm is shown. It is assumed that SR is polarized in the plane

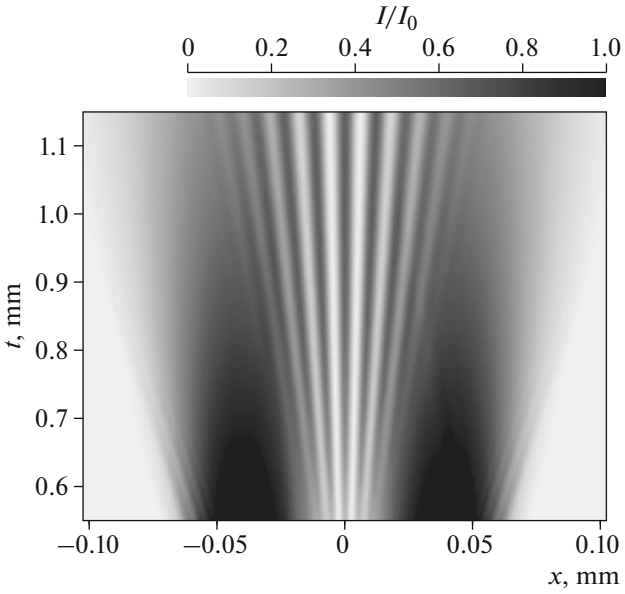

Fig. 3. Two-dimensional distribution map of the relative intensity in the reflected beam with the reflector crystal disregarded, at different thicknesses t of the second crystal. Calculation parameters were given in the text. $Z = 5$ m; $I_0 = 0.035$, provided that the intensity at the detector without crystals is unity.

oriented perpendicular to the diffraction plane. At the aforementioned parameter values, $\theta_B = 7.12°$.

Since absorption in a crystal leads to a decrease in intensity with an increase in the crystal thickness, all values of relative intensity above the specified value I_0 were replaced with I_0 to increase the contrast, which effectively corresponds to going beyond the dynamic measurement range of the detector. In Fig. 3, the I_0 value is chosen as half maximum of the value, which occurs at the smallest crystal thickness. Note that $I_0 = 0.023$ if the intensity at the detector without crystals is assumed to be unity.

One can see interference fringes of two types in the figure. The first ones are at the edges of the Borrmann fans for each beam at a small thickness t_2 of the second crystal. They have a variable period and correspond to interference of weakly and strongly damped wave fields at diffraction of a spherical wave and a small distance from source to crystal. These fringes were studied in 1961 [11, 12]. They disappear with an increase in the crystal thickness because of the absorption of strongly damped wave field.

Second-type fringes are located at the center of the pattern at large t_2 values. Low-absorption wave fields from different sources interfere in this region. Hence, they do not disappear at the center of the pattern even at large thicknesses of the second crystal. This interference is similar to that observed in Young's experiment. However, two sources were formed in the air gap because the crystal adds a reflected wave to the

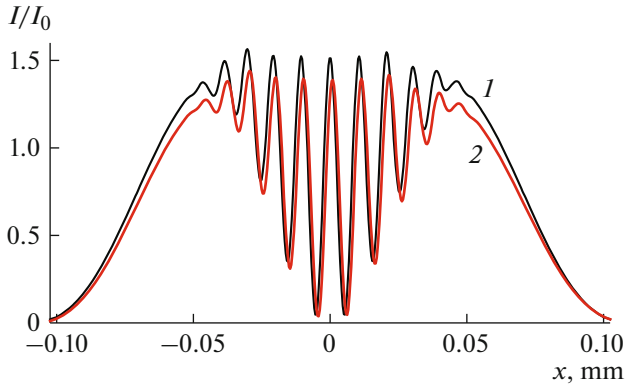

Fig. 4. Relative intensity distribution in the reflected beam for the parameters given in Fig. 3 at the second-crystal thickness of 1 mm. Curves *1* and *2* were obtained in the calculations with the reflector crystal disregarded and taken into account, respectively. The I_0 value is 0.01 of the intensity at the detector without crystals.

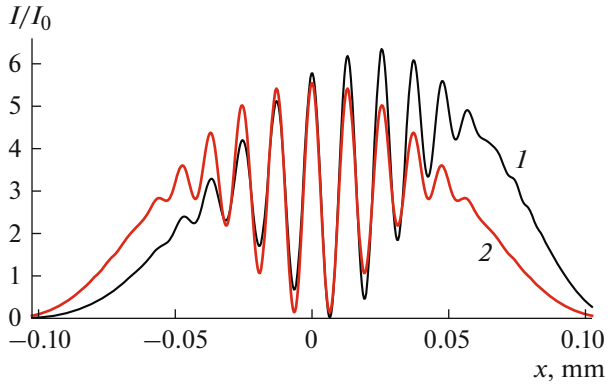

Fig. 5. Relative intensity distribution in the (*1*) direct and (*2*) reflected beams for the small distance $Z = 0.1$ m at equal thicknesses of the first and second crystals ($t_2 = t_1 = 0.5$ mm) and the air gap thickness of $t_g = 0.2$ mm. The I_0 value is 0.0001 of the intensity at the detector without crystals.

transmitted wave. The period of these fringes is proportional to the crystal thickness and corresponds to the formula derived in [13] (see Introduction).

In the calculation with allowance for the reflector crystal, mounted at the exact reflection position, interference fringes at large thicknesses barely change. Only a very weak shift (by small fractions of the period) of the fringes to the right is observed. At the same time, the fringes at the edges of the Borrmann fans are significantly blurred. The reason is that the reflector crystal bounds the angular radiation range all the same, which leads to reduction of high-frequency changes in the intensity pattern.

The above-described situation is illustrated in Fig. 4, where one can see the intensity distribution at the second-crystal thickness of 1 mm. Note that the black curve is obtained in the calculation with reflector crystal disregarded and completely corresponds to the cross section in Fig. 3. Curve *2* is obtained with allowance for the reflector crystal. One can see that the intensity slightly decreases because of the incomplete reflection by the third crystal. In addition, interference fringes are slightly shifted on the whole to the right. This displacement is not crucial; what is more important is that the fringe period is retained.

It is of interest that, if the reflector crystal is moved away from the exact reflection position, the reflected-beam intensity sharply decreases, while the contrast is deteriorated. Therefore, the crystal must be properly aligned. However, the angular width of the reflection region is quite sufficient for reproducing almost entire interference pattern.

The second case corresponds to a small distance Z from the secondary source to the crystal (specifically, 0.1 m). The diffraction focusing effect is completely absent at this distance. An advantage of this scheme is that one can deal without very thick crystals; therefore, the absorption loss is low. The point is that the air-layer thickness should be increased to reduce the oscillation period. At the same time, it is desirable to obtain beams with a maximally large width so as to make them intersect. In the above-described scheme, all processes occur in the second crystal; in contrast, the first crystal contracts the beams.

In the scheme with the minimum distance, both crystals cause beam divergence; therefore, the beams intersect at smaller thicknesses of the second crystal. It will be shown in the next section that the best interference in this scheme is achieved at equal thicknesses of the first and second crystals ($t_2 = t_1$). Figure 5 presents curves of relative intensity in the (*1*) direct beam and (*2*) reflected beam for the following parameters: $Z = 0.1$ m, $t_2 = t_1 = 0.5$ mm, and $t_g = 0.2$ mm. The I_0 value is equal to 0.0001 of the intensity at the detector without crystals. Such a small value is due to the fact that the Borrmann effect occurs in a significantly limited angular region, which corresponds to a large distance.

One can see that nine interference fringes, whose contrast rapidly decreases while moving away from the center to the edges of the beam intersection region, can be obtained at relatively small crystal thicknesses. The fringe period can be given by the formula presented in the Introduction if the crystal thickness is replaced with a sum of the thicknesses of two crystals. This formula will be derived from the calculation formulas in the next section. Note that a different derivation was given in [13]. Along with the period, the width of the intersecting beams is also an important parameter; a formula for its estimation will also be given below.

ANALYTICS. FRINGE PERIOD AND BEAM WIDTH

Let us consider the simplest and most interesting case: a slit with a very small size, a very small distance, and $t_1 = t_2 = t$. Note that the Fourier transforms of the WF after the slit and the Fresnel propagator can be assumed to be unity (it is sufficient to consider only the crystals). The angular dependence of the WF of the reflected beam $\psi_1(q)$ consists of two terms, which have the forms $M_{10}M_{00}$ and $M_{11}M_{10}$ in the absence of air layer. If there is an air layer with a thickness t_g, each of the two terms acquires a specific additional phase factor. As a result, we have

$$\begin{aligned}\psi_1(q) = M_{10}(q,t)M_{00}(q,t)\exp(-iqx_g)\\ + M_{11}(q,t)M_{10}(q,t)\exp(iqx_g),\end{aligned} \quad (14)$$

where $x_g = t_g\sin(\theta_B)$. The matrix elements $M_{ik}(q, t)$ are calculated from formulas (5)–(10).

Note that parameter G by definition has a negative real part. The parameter A also has a negative real part. Let the thickness t be so large that the Borrmann effect is implemented. In this case, the function E_p is much smaller than the function E_m and can be equated to zero. Then formula (14) can be rewritten in the form

$$\psi_1(q) = F(q)E_m^2(q)[\exp(iqx_g) + r^2\exp(-iqx_g)], \quad (15)$$

$$F(q) = -X_h/(2g(1 + r^2)). \quad (16)$$

The WF in real space is equal to the Fourier integral of the expression

$$\psi_1(x) = \int (dq/2\pi)\exp(iqx)\psi_1(q). \quad (17)$$

With allowance for (7), we have two terms in the integral. Let us consider the first one, $\psi_{11}(x)$. Here, the most rapidly varying factor in the integrand is exponential. It rapidly oscillates; therefore, the integral can be estimated by the stationary phase method.

The essence of the method is that the main contribution to integral (17) is from the region near the point q_0, where the phase $\varphi(q)$ of the exponential is almost constant (i.e., the phase derivative is zero). Furthermore, the following approximations are made: the factor before the exponential is replaced with a constant equal to the value at this point, and only zero and second terms of the power series in q are taken into account in the phase $\varphi(q)$ in the vicinity of this point, because the first term is zero:

$$\varphi(q) = \varphi(q_0) + (1/2)\varphi''(q_0)(q - q_0)^2. \quad (18)$$

Here, $\varphi''(q_0)$ means the second derivative of $\varphi(q)$ at point q_0.

The integral of this function is calculated analytically and equals to

$$\begin{aligned}\psi_{11}(x) = F(q_0)\left|E_m^2(q_0)\right|(2\pi\varphi''(q_0))^{-1/2}\\ \times\exp(i\varphi(q_0) + i\pi/4).\end{aligned} \quad (19)$$

It follows from the above formulas that the phase is

$$\varphi(q) = -2\,\mathrm{Im}(G(q)) + q(x + x_g). \quad (20)$$

Here, it is taken into account that $\mathrm{Re}(A(q))$ leads to a shift of the entire pattern as a whole in an undesirable direction. It was assumed to be zero in the numerical calculation to obtain a symmetric dependence relative to the origin of coordinates. Therefore, it is also omitted in this calculation. At the same time,

$$\begin{aligned}\mathrm{Im}(G(q)) = -t\sin(\theta_B)(q^2 + q_a^2)^{1/2},\\ q_a = \mathrm{Re}(X)/\sin(2\theta_B).\end{aligned} \quad (21)$$

The sign depends on the way of determining the sign of $\mathrm{Re}(X)$. It is chosen provided that $\mathrm{Re}(X) > 0$.

Since the scheme operates under the Borrmann conditions, one cannot deviate significantly from the point $q = 0$ (otherwise the absorption would rapidly increase). We assume that $q_0 \ll q_a$. Then, instead of (20), we find approximately that

$$\varphi(q) = 2t\sin(\theta_B)q_a(1 + q^2/(2q_a^2)) + q(x + x_g). \quad (22)$$

The following solution is obtained from the equation $\varphi'(q) = 0$:

$$\begin{aligned}q_0 = -q_a(x + x_g)/(2t\sin(\theta_B)),\\ \varphi''(q_0) = t\sin(\theta_B)/q_a,\end{aligned} \quad (23)$$

$$\begin{aligned}\varphi(q_0) = \varphi_0 - q_a(x^2 + x_g^2 + 2xx_g)/(4t\sin(\theta_B)),\\ \varphi_0 = 2t\sin(\theta_B)q_a.\end{aligned} \quad (24)$$

The term in the phase of the function $\psi_{11}(x)$, which changes sign with a change in the sign of x_g, is of interest. In addition, we generally have $t_g \ll 2t$ and $r^2 \approx 1$ in the central part of the interference pattern.

Taking into account the aforementioned approximations, the sum of the two contributions to the WF of the reflected beam at the center can be written as

$$\psi_1(x) = A(x, x_g)\cos(xx_gq_a/(2t\sin(\theta_B))). \quad (25)$$

The magnitude of this function oscillates with a period $2p$, and the intensity (i.e., squared magnitude) oscillates with a period p, where

$$p = \lambda t\sin(2\theta_B)/(|\chi_h|t_g). \quad (26)$$

Here, (9) and (21) are taken into account, and the x axis (as in the calculation formulas) is oriented perpendicular to the beam direction. While moving away from the center to the edges of the interference pattern, r^2 decreases, and the contrast becomes incomplete and then disappears at all. One can easily understand from the presented derivation that the average

value $t = (t_1 + t_2)/2$ should be used if the thicknesses of two crystals are not equal.

Another important parameter is the beam width in space under the Borrmann conditions. At small crystal thicknesses (when the absorption is of minor importance), a narrow beam exposes the Borrmann fan with a base width of $2t\sin(\theta_B)$ in the direction perpendicular to the beam direction. However, absorption reduces the width beam. At very large crystal thicknesses, the intensity profile under the Borrmann conditions has a Gaussian shape with the half-width

$$W = (C_w \lambda t/|\chi_{ih}|)^{1/2}, \quad C_w = (4\ln 2/\pi)\sin(\theta_B)\sin(2\theta_B). \tag{27}$$

Derivation of this formula in the general case of asymmetric diffraction was given in [14]; a particular case of symmetric diffraction and sigma polarization is presented in (27). Here, $t = (t_1 + t_2)/2$ (as above). The parameter χ_{ih} is a Fourier component of the imaginary part of crystal polarizability.

In fact, the WFs of two beams interfere, and we are interested in the half-width of the curve describing the WF magnitude. It is wider by a factor of $2^{1/2} = 1.414$. Note that formula (27) yields a correct value (consistent with the numerical calculation) only at crystal thicknesses larger than 5 mm for the parameters under consideration. At smaller thicknesses, the values are overestimated. For example, for a thickness of 1 mm, it gives a value that is larger by a factor of 1.4 than that calculated numerically.

CONCLUSIONS

Diffraction of X rays in a crystal under the Borrmann conditions forms two beams with approximately identical properties. The air gap between two crystal blocks separates beams in space, and the intersection of the beams in the second block leads to their interference. The most interesting situations arise in two cases: (i) when implementing diffraction focusing of the beams in the first block and (ii) at zero distance between the secondary source (slit) and the block of two crystals.

A method for calculating this interference was developed, the results of numerical simulation were presented, and analytical formulas for the radiation intensity oscillation period and beam widths were derived. The interferometer has spectral stability and allows one to obtain precise values of diffraction parameters and refractive indices of any materials, which can be placed on the beam path in the air gap.

The oscillation period is proportional to the part of the summary thickness of crystal blocks that is located after the focusing thickness. This part equals to the second-block thickness in the first case and to the total thickness of two blocks in the second case.

REFERENCES

1. M. Born and E. Wolf, *Principles of Optics* (Cambridge Univ. Press, Cambridge, 2002). ISBN-13: 978-0521642224; ISBN-10: 0521642221
2. A. Snigirev, I. Snigireva, V. Kohn, et al., Phys. Rev. Lett. **103** (064801) (2009). https://doi.org/10.1103/PhysRevLett.103.064801
3. A. Snigirev, I. Snigireva, V. Kohn, et al., AIP Conf. Proc. (10th Int. Conf. Xr. Micr) **1365**, 285 (2011). https://doi.org/10.1063/1.3625360
4. A. Snigirev, I. Snigireva, M. Lyubomirskiy, et al., Optics Express, **22**, 25842 (2014). https://doi.org/10.1364/OE.22.025842
5. M. Lyubomirskiy, I. Snigireva, V. Kohn, et al., J. Synchrotron Radiat. **23**, 1104 (2016). https://doi.org/10.1107/S160057751601153X
6. D. Zverev, I. Snigireva, V. Kohn, et al., Optics Express **28**, 21856 (2020 https://doi.org/10.1364/OE.389940
7. D. A. Zverev, V. G. Kohn, V. A. Yunkin, et al., Proc. SPIE **11493**, 114930L1 (2020). https://doi.org/10.1117/12.2568687
8. A. Snigirev, V. Kohn, I. Snigireva, and B. Lengeler, Nature **384**, 49 (1996). https://doi.org/10.1038/384049a0
9. V. V. Lider, Usp. Fiz. Nauk **184**, 1217 (2014). https://doi.org/10.3367/ufne.0184.201411e.1217
10. N. Kato and A. R. Lang, Acta Crystallogr. **12**, 787 (1959). https://doi.org/10.1107/S0365110X59002262
11. N. Kato, Acta Crystallogr. **14**, 526 (1961). https://doi.org/10.1107/S0365110X61001625
12. N. Kato, Acta Crystallogr. **14**, 627 (1961). https://doi.org/10.1107/S0365110X61001947
13. M. K. Balyan, Acta Crystallogr. A **66**, 660 (2010). https://doi.org/10.1107/S0108767310035944
14. A. M. Afanas'ev and V. G. Kohn, Sov. Phys. Solid State **19** (6), 1035 (1977).
15. V. G. Kon, Kristallografiya **24**, 712 (1979).
16. A. A. Aristov, V. I. Polovinkina, I. M. Shmyt'ko, and E. V. Shulakov, Pis'ma Zh. Eksp. Teor. Fiz. **28**, 6 (1978).
17. V. D. Koz'mik and I. P. Mikhailyuk, Pis'ma Zh. Eksp. Teor. Fiz. **28**, 673 (1978).
18. V. V. Aristov, V. I. Polovinkina, A. M. Afanasev, and V. G. Kohn, Acta Crystallogr. A **36**, 1002 (1980). https://doi.org/10.1107/S0567739480002045
19. V. V. Aristov, V. G. Kohn, and A. A. Snigirev, Sov. Phys. Crystallogr. **31** (6), 626 (1986).
20. V. V. Aristov, A. A. Snigirev, A. M. Afanasev, et al., Acta Crystallogr. A **42**, 426 (1986). https://doi.org/10.1107/S0108767386098926
21. V. G. Kohn, O. Y. Gorobtsov, and I. A. Vartanyants, J. Synchrotron Radiat. **20**, 258 (2013). https://doi.org/10.1107/S0909049513000903

22. V. G. Kohn, I. A. Smirnova, I. I. Snigireva, and A. A. Snigirev, Crystallogr. Rep. **63**, 536 (2018).
23. V. G. Kohn, I. A. Smirnova, I. I. Snigireva, and A. A. Snigirev, Crystallogr. Rep. **63**, 536 (2018). https://doi.org/10.1134/S1063774518040119
24. V. G. Kohn and I. A. Smirnova, Acta Crystallogr. A **74**, 699 (2018). https://doi.org/10.1107/S2053273318012627
25. V. G. Kohn, I. Snigireva, and A. Snigirev, Phys. Status Solidi **222**, 407 (2000). https://doi.org/10.1002/1521-3951(200011)222:2<407::AID-PSSB407>3.0.CO;2-X
26. A. Authier, *Dynamical Theory of X-ray Diffraction* (Oxford Univ. Press, 2005). ISBN: 9780198528920
27. Z. G. Pinsker, *Dynamical Scattering of X-Rays in Crystals* (Springer, 1978). ISBN: 978-3-642-81209-5
28. V. G. Kohn, Phys. Status Solidi B **231**, 132 (2002). https://doi.org/10.1002/1521-3951(200205)231:1<132::AID-PSSB132>3.0.CO;2-C
29. V. G. Kohn, http://kohnvict.ucoz.ru/jsp/3-difpar.htm.
30. V. G. Kohn, http://kohnvict.ucoz.ru/acl/acl.htm.
31. J. W. Cooley and J. W. Tukey, Math. Comput. **19**, 297 (1965).
32. https://www.nag.co.uk/content/nag-library-fortran.

Translated by Yu. Sin'kov